Transactions of the Korean Nuclear Society Spring Meeting

Gyeongju, Korea, October 29-30, 2026

Screening of Latent and Sensible Heat Storage Media for a Packed Bed Passive Containment Condenser

Hyochan Kim, Jeong Ik Lee*

Department of Nuclear and Quantum Engineering, Korea Advanced Institute of Science and Technology, 373-1 Guseong-dong Yuseong-gu, Daejeon 305-701, Republic of Korea

** Corresponding author: jeongiklee@kaist.ac.kr*

Keywords: Passive Containment Cooling, Phase Change Materials, Volumetric Heat Capacity

1. Introduction

Fukushima Daiichi nuclear accident of 2011 shifted engineers' attentions to passive safety systems (PSS), systems that do not rely on external power supplies to operate. Among different concepts, an approach using phase change materials (PCMs) as a heat sink to containment building is drawing more attention due to its large latent heat of fusion, which is several times larger than the sensible heat over a narrow temperature interval [1]. Since the melting temperature can be selected by material choice, PCM will be present in the containment during normal operation, and start melting when temperature rises during an accident. If steam is released to the containment, the steam contacts with the PCM cooling system and condense at its surface, absorbing energy directly and limiting the pressure rise. The configuration considered here is a packed bed of small pebbles, shown in Fig. 1: a metal shell containing the PCM together with a void that accommodates expansion on melting. Steam reaching the bed condenses on the outer surfaces, and heat conducts inward through the shell, driving a melt front toward the pebble center. How much energy a pebble absorbs within the accident window is therefore governed not only by the properties of the PCM, but also by how far that front travels.

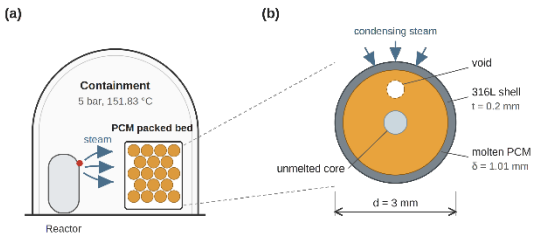


Figure 1. (a) PCM packed bed as an in-containment heat sink (b) Cross-section of a single pebble at the end of the mission time

The conventional argument for PCM is made on energy density (by mass) basis, as it is much higher than that of non-PCMs that only utilize sensible heat. However, mass is not the binding constraint in a containment building. Free volume is fixed in containment building; any absorber installed within it displaces volume and raises the pressure when gas is released. The governing metric is energy absorbed per unit volume, and three aspects have to be considered for PCM. The shell and the void inside each pebble both consume volume that would otherwise hold PCM. In addition, the thermal conductivity of PCMs is very low compared with metals, so the melt front advances only a short distance within a brief accident window, and latent heat held in the pebble core may never be reached.

Volumetric energy density of encapsulated PCM has been treated as a material selection criterion [2], and shell thickness has been optimized for storage density and heat transfer rate [3]. Both target repeated charging duty and compare PCM configurations against one another. Neither the fraction of a pebble that melts within a fixed accident window, nor the question of whether encapsulation is worthwhile relative to a bare pebble of the shell material, has been used as a screening criterion. This paper screens eight candidate media on energy absorbed per unit volume, at a pebble geometry derived from the accident timescale, to establish whether the per mass advantage of PCM survives once these penalties are applied. The comparison addresses thermal capacity only; the rate at which that capacity is delivered is a separate criterion and is not evaluated here.

Nomenclature

α – thermal diffusivity	P_{cr} – critical buckling pressure
β_l – liquid volumetric expansivity	ρ – density
c_p – specific heat capacity	Q – heat energy
δ – melt front penetration depth	R_c – PCM core radius
d – pebble diameter	Ste – Stefan number
E – Young's modulus	t – shell thickness
f_{melt} – melted fraction of PCM	T – temperature
f_{sens} – sensible utilization factor	τ – time
h_{sl} – latent heat of fusion	V – volume
K – bulk modulus	λ – root of Stefan equation
k – thermal conductivity	ϕ – volume fraction
m – design margin	ν – Poisson's ratio

2. Analysis Framework

2.1 Reference scenario and thermal envelope

The containment is assumed to be at 5 bar, corresponding to the design pressure of a large pressurized water reactor such as APR-1400. Normal operating temperature in containment is at 55℃ [4]. Non-condensable gas (NCG) is assumed to be neglected, so that the steam is at the saturation temperature (151.83℃) which condenses at the surface, giving a temperature swing of ΔT = 96.83K. Neglecting NCG places the condensing rate at the highest it could reach, as presence of NCG hinders the heat transfer from steam to surface, giving the largest temperature swing. This works against PCM rather than for it: sensible capacity grows in proportion to ΔT while the latent contribution is fixed, so a larger swing narrows the margin between the two. Thus, if PCM performs better in no-NCG condition, then the results will not change with NCG added. A mission time of 5s is adopted, corresponding to the period over which peak pressure develops and within which absorbed energy contributes to mitigating it.

Eight candidate media were chosen, which is shown in Table 1: two organic, two inorganic PCMs, and 4 sensible media (property values are taken from manufacturer data sheets where available and from literature otherwise). Organic PCMs, like paraffin or fatty acids, are generally chemically more stable, free of phase segregation, and non-corrosive, but they also have lower thermal conductivity and density. Inorganic PCMs have higher thermal conductivity and volumetric energy density, but are corrosive and have risks of supercooling and phase segregation. Lastly, sensible media store heat only when temperature rises, but their thermal diffusivity is two to three orders of magnitude above that of PCMs, so a sensible pebble heats essentially uniformly within the mission time.

2.2 Pebble geometry and encapsulation

A sensible pebble can be manufactured from a single material, but PCM pebble cannot; it has to be encapsulated and sealed. Molten PCM would otherwise drain from the bed and destroy the packed geometry. Also, the inorganic candidates are corrosive toward containment structures, and sealing is what retains the water of hydration within the salt hydrates. The bed geometry is a packed bed, so a spherical pebble of outer diameter d and shell thickness t is analyzed:

$$\phi_{shell} = 1 - \left(1 - \frac{2t}{d}\right)^3 \quad \dots (1)$$

The shell is composed of 316L stainless steel, chosen for three reasons. Immersion tests on metal-salt hydrate pairs at storage temperatures found stainless steel compatible with sodium acetate trihydrate while brass and copper were not. [5] Aluminum is excluded on a nuclear-specific basis: it is amphoteric and produces hydrogen in the alkaline conditions of post-accident containment water, which is why aluminum inventory in containment is controlled [6], whereas stainless steel does not present the same hydrogen generation and chemical effect concerns. Finally, 316L has the highest volumetric heat capacity of the candidate shell metals.

The shell is treated as thermally active as it occupies part of the installed volume, and its thermal diffusivity is high enough to equilibrate fully within the mission time.

2.3 PCM pebble void fraction

On melting, the PCM expands, and the liquid expands further as it is heated to the peak surface temperature. A sealed pebble must therefore contain a void, or the liquid will pressurize against a rigid shell. The required void has two contributions, volume change on melting and the thermal expansion of the liquid. With design margin m:

$$\phi_{void} = \left(\frac{\rho_s}{\rho_l} - 1\right) + \beta_l(T_{sat} - T_m) + m \quad \dots (2)$$

A design margin of 0.05 is added. The molten salt hydrate is nearly incompressible, and excess liquid volume must be accommodated almost entirely by compression. Treating the liquid and the shell as compliances in series gives an effective bulk modulus [7]:

$$\frac{1}{K_{eff}} = \frac{1}{K_l} + \frac{3R(1-\nu)}{2tE}$$

and pressure is calculated by multiplying overfill fraction f [7]:

$$p = K_{eff} f$$

A volumetric overfill of 1% would generate an internal pressure of ~200 bar and a membrane stress of 76 MPa. Since the quoted densities in Table 1 carry tolerances of up to 10%, margin is sized to prevent pebble from being overfilled.

2.4 Volumetric energy density

For a sensible storage medium, the energy absorbed per unit volume only changes based on temperature change. Density and specific heat capacity are taken as constant. Then, energy change per volume over a swing of ΔT is:

	Type	Name	T_m (℃)	ρ_s (kg/m^3)	ρ_l (kg/m^3)	$c_{p,s}$ (kJ/kg·℃)	$c_{p,l}$ (kJ/kg·℃)	h_{sl} (kJ/kg)	k_s (W/m·K)	k_l (W/m·K)
PCM	Organic	Paraffin [8]	58	880	808	2	2	140	0.2	0.2
	Organic	PEG 6000 [9]	60	1,200	1,070	2	2	185	0.35	0.35
	Inorganic	Climsel C58 [10]	58	1,480	1,400	4	3	265	0.57	0.47
	Inorganic	savE HS58 [11]	58	1,400	1,320	2.40	3.15	267	0.61	0.51
Metal	-	Stainless 316L [12]	-	8,238	-	0.468	-	-	13.4	-
	-	Carbon Steel (AISI 1010) [12]	-	7,832	-	0.434	-	-	63.9	-
	-	Aluminum [12]	-	2,702	-	0.903	-	-	237	-
Ceramic	-	Al_2O_3 (99%) [12]	-	3,890	-	0.88	-	-	35	-

Table 1. Thermodynamic properties of varying materials used

$$\frac{Q_s}{V} = \rho_s c_{p,s} \Delta T \ \dots (3)$$

The thermal diffusivity of metals is two to three orders of magnitude above that of PCMs. Fourier number for alumina at d = 3mm is roughly 18.9, meaning pebble is fully equilibrated with its surface well within the accident window.

For an encapsulated PCM whose melting point T_m lies within the swing, the corresponding expression would have to separate the shell part, solid and liquid phase, while including latent heat. Taking the fractions from equations (1) and (2):

$$\frac{Q_p}{V} = (1-\phi_{shell})(1-\phi_{void})\rho_p\left[f_{sens}\bar{c_p}(\Delta T - \Delta T_{band}) + f_{melt}h_{sl}\right] + \phi_{shell}\rho_{shell}c_{p,shell}\Delta T \ \dots (4)$$

$$* \ \bar{c_p} = \frac{T_m - T_0}{\Delta T}c_{p,s} + \left(1 - \frac{T_m - T_0}{\Delta T}\right)c_{p,l}$$

$$* \ f_{sens} = 1 - \frac{6}{\pi^2}\sum_{n=1}^{\infty}\frac{1}{n^2}\exp\left(-n^2\pi^2\frac{\alpha\tau}{R_c^2}\right)$$

$$* \ \Delta T_{band} = T_{band,upper} - T_{band,lower}$$

$$* \ f_{melt} = 1 - \left(1 - \frac{\delta}{R_c}\right)^3$$

c_p correction ($\bar{c_p}$) was used to account for manufacturer's latent heat measurement. Both inorganic PCMs were measured using T-history method over a finite temperature band rather than at a single point. In this method, the enthalpy change is integrated over a finite temperature band, ΔT_{band} (53-62℃ for savE, 49-64℃ for Climsel), as the sample is heated through the transition. The reported enthalpy, h_{sl}, is therefore not a pure latent heat and already contains the sensible heat within that band. Adding $\bar{c_p}\Delta T$ across the full range would count the sensible contribution twice, so the overlap is therefore subtracted.

All of PCM may or may not melt within the given duration of accident window; it depends on the given time, rate of melting, and mass of PCM in each pebble. The amount of melt PCM in a given period of time, f_{melt}, can be determined by calculating the melt front position δ, which can be obtained from the one-dimensional Stefan solution: the heat equation in liquid layer, with the wall held at T_{sat}, the interface at T_m, and the Stefan condition are used below [13].

$$k_l\frac{\partial T}{\partial x} = \rho h_{sl}\frac{\partial \delta}{\partial \tau}$$

$$\delta = 2\lambda\sqrt{\alpha\tau}$$

$$* \ \lambda e^{\lambda^2}\operatorname{erf}\lambda = \frac{Ste}{\sqrt{\pi}}$$

$$* \ Ste = \frac{c_{p,l}(T_{sat} - T_m)}{h_{sl}}$$

The sensible utilization, f_{sens}, is treated separately from f_{melt}, because heat conducts ahead of the phase front and the unmelted core also rises in temperature up to T_m. It is the fractional energy uptake of a sphere initially at T_0 whose surface is stepped to T_{sat}, obtained by separation of variables with a symmetry condition at the center, using transient conduction solution for a sphere with a step change in surface temperature [14]. For the two salt hydrates considered, T_m lies only 3K above T_0, so the solid core can contribute at most ~7 kJ kg^{-1} against a total near 540 kJ kg^{-1}. Essentially all of the sensible contribution is taken up by molten PCM above the melting point.

3. Reference pebble geometry

Comparing media on a volumetric basis requires a common capsule geometry, and that geometry cannot be assumed, because different materials outperform each other depending on operating conditions. This section establishes the geometry at which the comparison of Section 4 is made.

The shell thickness determines shell's volumetric occupation, which relates to overall volumetric energy

storage capacity of a pebble. If we rewrite the equation (4) as a volume-weighted mixture of the PCM core and the shell:

$$\frac{Q}{V} = (1-\phi_{shell})q_p + \phi_{shell}q_{shell} \quad \cdots (5)$$

$$* (1-\phi_{shell}) = \left(\frac{R_c}{d/2}\right)^3$$

$$* q_p = (1-\phi_{void})\rho_p\left[f_{sens}\bar{c_p}(\Delta T - \Delta T_{band}) + f_{melt}h_{sl}\right]$$

$$* q_{shell} = \rho_{shell}c_{p,shell}\Delta T$$

In this form, the pebble is a mixture of two absorbers and Q/V is the volume-weighted average of their energy densities. The two geometric parameters behave differently: Q/V is monotonic in shell thickness but has an interior maximum in diameter.*3.1 Shell thickness*

Since the shell volume fraction, for a fixed diameter, monotonically decreases as thickness decreases, the optimum is when t is minimum. To identify the lower bound, structural integrity is analyzed. During the accident, the external pressure could cause sphere to fail by buckling, for which the classical elastic buckling pressure of a thin spherical shell is used [15]:

$$P_{cr} = \frac{2Et^2}{R^2\sqrt{3(1-\nu^2)}}$$

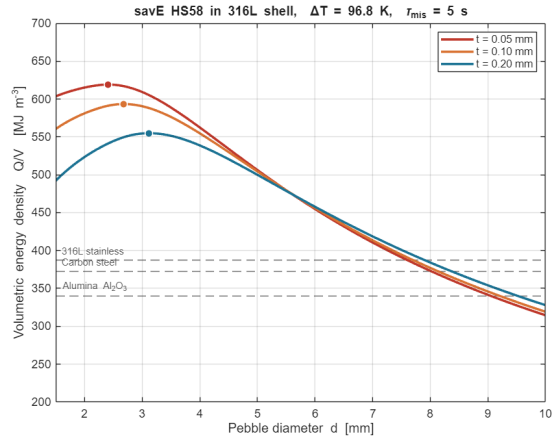


Figure 2. Shell thickness comparisons for varying pebble diameterFor Stainless 316L, its values are E = 190 GPa, v = 0.29 at 152°C (5 bar). Accounting for 0.2 knockdown factor, since spheres are reported to buckle at 20-30% of classical value due to tiny geometric imperfections [16], a wall of ~5.0 μm is sufficient for the bounding case of the full 5 bar acting across the shell. Since the actual pressure difference across the shell is smaller than this bounding value, structural requirement is not binding. It is rather the manufacturing capability that sets the lower bound. Reported macro-encapsulation of PCM has diameter range of 10-50 mm and shell thickness 1-2 mm [17], so proportionally, t = 0.2 mm is adopted here on that basis.

3.2 Pebble diameter

For diameter, the two effects compete. It is convenient to work in terms of the PCM core radius, R_c, since at fixed shell thickness, volumetric energy density depends on the geometry only through R_c. Increasing R_c with fixed t raises the PCM volume fraction, but reduces both utilization factors. The melt front advances only 1.01 mm in 5 s mission time for savE HS58 according to Stefan solution, independent of capsule size, so a larger core simply leaves more PCM solid. f_{sens} falls because the Fourier number decreases, leaving the pebble further from thermal equilibrium at the end of the mission. Differentiating Eq. (5) with respect to core radius:

$$\frac{d\left(\frac{Q}{V}\right)}{dR_c} = \frac{d(1-\phi_{shell})}{dR_c}(q_p - q_{shell}) + (1-\phi_{shell})\left(\frac{dq_p}{dR_c}\right) = 0 \quad \cdots (6)$$

$$* \frac{d(1-\phi_{shell})}{dR_c} = \frac{3R_c^2 t}{(R_c+t)^4} > 0, \qquad \frac{dq_p}{dR_c} < 0$$

The first term is gain from displacing less shell, and the second is the loss from leaving more of the core un-melted. The optimum is where the two effects cancel each other, which the weighted contributions balance.

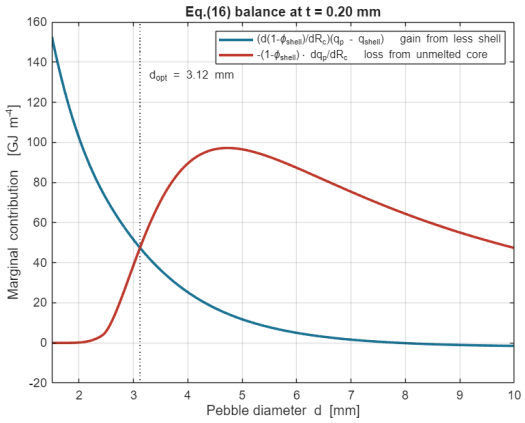


Figure 3. Optimum diameter for a pebble encapsulated with t=0.2mm thickness

Solving Eq. (6) numerically gives d_{opt} = 3.12 mm as shown on Figure 2. The optimum shifts with shell thickness; diameter decreases as thickness decreases, and increases as thickness increases. Since the melt front is 1.01 mm at 5s, R_c is roughly 1.35δ, and 99% of the PCM melt. At d = 3 mm, the volumetric energy capacity is 554.6 MJ m^{-3} compared to 554.9 MJ m^{-3} at

3.12 mm; for engineering purposes, d = 3 mm will be adopted. Under-sizing would result in PCM core being fully melted but volume fraction would be lost to shell. Oversizing on the other hand sees larger un-melted volume fraction, meaning the latent heat was not fully utilized during the accident scenario.

4. Volumetric energy capacity comparison

All media are evaluated at the reference condition of Section 2.1 and at the pebble geometry established in Section 3 was plotted for varying ΔT in Figure 3. At ΔT = 96.83K point, the two inorganic salt PCMs are indistinguishable, and both exceeded the best sensible medium by a far margin. This follows from their high specific heat capacity as much as from their latent heat. The organic PCMs do not perform as comparably: PEG 6000 falls marginally below the solid 316L pebble, and paraffin reaches ~70% below PEG 6000. Among the sensible media, the ranking follows ρc_p directly and aluminum is weakest despite its high specific heat because is one third of stainless steel.

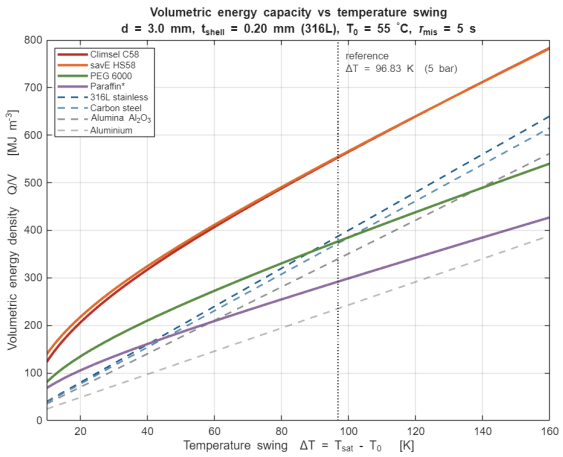


Figure 4. Volumetric energy density for different materials at varying ΔT

If latent heat was not present, then the graph looks like Figure 4. All PCM materials fall below solid 316L reference, which shows that PCM's sensible properties are not favorable compared to metal and that stainless shell that occupies 35% of the pebble volume is not favorable. Without phase change, encapsulation does not have advantages. The latent contribution exceeds the entire margin over the reference pebble.

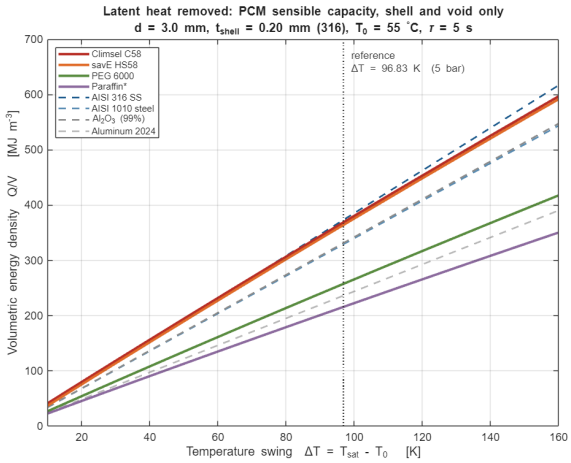


Figure 5. Volumetric energy density excluding latent heat for different materials at varying ΔT

Because a pebble is a volume weighted mixture of two absorbers, Eq (5), encapsulation improves on a solid pebble of the shell material only when the PCM core outperforms the shell it displaces. Comparing the intrinsic PCM core density q_p at full utilization against q_{shell} gives a single screening criterion, independent of capsule geometry.

The salt hydrates carry a 76% margin over the shell, so encapsulation is clearly worthwhile. PEG 6000 is marginal at 1.06: at 3 mm the melt front reaches only 94% of the PCM core, its effective PCM core density falls below q_{shell}, and the capsule drops just below the solid reference. Paraffin fails the criterion outright. With q_p/q_{shell} = 0.65, a stainless shell absorbs more energy than paraffin it contains at any diameter, and no capsule geometry can recover the deficit. This also reverses the conclusion of Section 3.1, which assumed $q_p > q_{shell}$ for PCMs, as for paraffin, a thicker shell would improve Q/V.

Figure 3 also shows that there is no best solution for the whole range of temperature swing. The latent contribution is set by h_{sl} and does not scale with ΔT, whereas sensible capacity is proportional to it, so the two organic PCMs are overtaken by the sensible media as the temperature difference grows. Paraffin falls below alumina at ΔT = 63K and below carbon steel at 65K, both below the reference condition. PEG 6000 crosses at ΔT = 152K and 156K respectively, above the reference condition, so it remains ahead of the sensible media at ΔT = 96.83K but would not at a higher design pressure. Neither organic falls to aluminum within the range examined, making aluminum the weakest medium considered. The inorganic salt hydrates show no such crossing within the range examined, because their volumetric heat capacity exceeds that of the sensible media even before the latent term is counted.

5. Discussion

From the comparison, inorganic salt hydrates are the best of the eight media considered, exceeding the strongest sensible candidate. The savE HS58 data sheet states a maximum operating temperature of 75℃ [11], against a peak surface temperature of 151.83℃ in the present duty, and neither salt hydrate is characterized above about 65℃. Salt hydrates lose water of crystallization on heating, which would destroy the latent heat capacity on which the result depends. In a sealed capsule however, the water cannot leave: it partitions between the liquid and the small vapor headspace, and the material becomes a hot concentrated solution rather than a dehydrated salt. The manufacturer's limit is therefore expected to apply to open or vented service rather than to the sealed capsule analyzed here. This expectation has not been verified experimentally and is the principal open question raised by this work.

Approximately 55% of the energy absorbed per unit mass by either salt hydrate comes from sensible heating of the liquid above the melting point, evaluated with a specific heat that the manufactures report at 60 to 65℃ [10][11] and applied here across a further 94 K. More than half of the reported advantage therefore rests on an extrapolated property, on a material characterized over a much narrower range. Compatibility data is similarly bounded: the immersion tests cited in Section 2.2 were conducted at 48 to 58℃ [5].

Several simplifications bear on the numbers reported. Properties are held constant over the swing and taken at 300 K, while the duty spans 328 to 425 K; the specific heat of carbon steel rises by approximately 12% [12] and that of alumina by 18% across this range, so the sensible baselines are understated. The melt front position is the one-dimensional planar Stefan solution applied to a sphere, exact only for $\delta << R_c$.

6. Conclusion

Eight candidate absorber media were compared to each other on energy absorbed per unit installed volume for a packed-bed passive condenser, at a pebble geometry. The per-mass advantage of PCM does not survive the change of basis: after accounting for shell, void, and incomplete melting, PCMs do not excel as well. Only the two inorganic salt hydrates outperform bare sensible pebbles at the reference condition. The margin is carried entirely by the latent heat. Every PCM falls below the solid reference with latent heat removed, so encapsulation is a net loss without it. This gives a screening criterion independent of geometry: encapsulation is worthwhile only where the PCM core outperforms the shell it displaces.

Three tasks follow directly. First, the thermal stability of the sealed capsule must be established experimentally. The salt hydrates are characterized only to about 65℃ and the rated 75℃, while the duty reaches 151.83℃, and the argument that a sealed capsule prevents dehydration is at present untested. The same measurements would supply the liquid specific heat at temperature, on which more than a half the reported advantage depends. Second, a rate-based comparison is required, since capacity and rate need not rank media in the same order. Third, the volumetric result must be closed with the containment response, because an absorber installed inside containment displaces gas from a fixed free volume and raises the pressure it is intended to suppress.

ACKNOWLEDGEMENT

This work was supported by KOREA HYDRO & NUCLEAR POWER CO., LTD (No. 8TH-TECH-01)

This research was supported by Basic Science Research Program through the National Research Foundation of Korea(NRF) funded by the Ministry of Education(No. RS-2025-25402679)

REFERENCES

[1] Sharma, A., Tyagi, V.V., Chen, C.R., Buddhi, D., "Review on thermal energy storage with phase change materials and applications," Renewable and Sustainable Energy Reviews, Vol. 13, No. 2, 2009, pp. 318-345. doi:10.1016/j.rser.2007.10.005[2]Otero, J.A., Santiago-Acosta, R.D., Pérez-Álvarez, R., Hernández-Cooper, E.M., "Volumetric and gravimetric energy densities of encapsulated high temperature phase change materials: Materials selection criteria," Applied Thermal Engineering, Vol. 274, 2025, 126448.

[3] Cáceres, G., Fullenkamp, K., Montané, M., Naplocha, K., Dmitruk, A., "Encapsulated Nitrates Phase Change Material Selection for Use as Thermal Storage and Heat Transfer Materials at High Temperature in Concentrated Solar Power Plants," Energies, Vol. 10, No. 9, 2017, p. 1318.

[4] KEPCO/KHNP, "APR1400 Design Control Document Tier 2, Chapter 6: Engineered Safety Features," Rev. 3, August 2018, Table 6.2.1-3. https://www.nrc.gov/docs/ML1822/ML18228A653.pdf

[5] Cabeza, L.F., Illa, J., Roca, J., Badia, F., Mehling, H., Hiebler, S., Ziegler, F., "Immersion corrosion tests on metal-salt hydrate pairs used for latent heat storage in the 48 to 58 °C temperature range," Materials and Corrosion, Vol. 53, 2002. doi:10.1002/maco.200290004

[6] U.S. Nuclear Regulatory Commission, "Standard Review Plan," NUREG-0800, Section 6.2.5, "Combustible Gas Control in Containment."

[7] Manring, N.D., "Fluid Properties," Hydraulic Control Systems, John Wiley & Sons, New York, 2005, Ch. 1.

[8] Thonon, M., Zalewski, L., Gibout, S., Franquet, E., Fraisse, G., Pailha, M., "Experimental Comparison of Three Characterization Methods for Two Phase Change Materials Suitable for Domestic Hot Water Storage," applied Sciences, Vol. 11, No. 21, 2021, p. 10229. doi:10.3390/app112110229

[9] Sharma, R.K., Ganesan, P., Tyagi, V.V., Mahlia, T.M.I., "Accelerated thermal cycle and chemical stability testing of polyethylene glycol (PEG) 6000 for solar thermal energy storage," Solar Energy Materials and Solar Cells, Vol. 147, 2016, pp. 235-239. doi:10.1016/j.solmat.2015.12.023

[10] Climator Sweden AB, "ClimSel C58 Product Data Sheet," Skövde, Sweden.

[11] PLUSS Advanced Technologies Pvt. Ltd., "savE® HS58 Technical Data Sheet," Gurugram, India.

[12] Bergman, T.L., Lavine, A.S., Incropera, F.P., DeWitt, D.P., "Appendix A: Thermophysical Properties of Matter," Fundamentals of Heat and Mass Transfer, 7th ed., John Wiley & Sons, Hoboken, NJ, 2011.

[13] Alexiades, V., Solomon, A.D., Mathematical Modeling of Melting and Freezing Processes, Hemisphere, Washington DC, 1993.

[14] Carslaw, H.S., Jaeger, J.C., Conduction of Heat in Solids, 2nd ed., Oxford University Press, Oxford, 1959.

[15] Zoelly, R., "Über ein Knickungsproblem an der Kugelschale," Dissertation, ETH Zürich, 1915.

[16] NASA, "Buckling of Thin-Walled Doubly Curved Shells," NASA SP-8032, Space Vehicle Design Criteria (Structures), 1969.\

[17] Höhlein, S., König-Haagen, A., Brüggemann, D., "Macro-Encapsulation of Inorganic Phase-Change Materials (PCM) in Metal Capsules," Materials, Vol. 11, No. 9, 2018, p. 1752.